Supplementary Information

Cooperative supramolecular integration of QS-21 into polymeric micelles as a tunable nanoadjuvant platform for subunit vaccines

Patricio Guillermo Márquez[a,b], Leonardo Gabriel Alonso[a,b], Juan Ignacio Marfía[c,d], Ignacio Smith[a,e], Ana Carolina Mourelle[c,d], María Lina Formica[f], María Victoria Miranda[a,b], Silvina Noemí Valdez[c,d], Federico Javier Wolman[a,b] and Romina Julieta Glisoni[a,b*]

[a]Universidad de Buenos Aires (UBA), Facultad de Farmacia y Bioquímica, Departamento de Microbiología, Inmunología, Biotecnología y Genética, Cátedra de Biotecnología, Junín 956, C1113AAD Buenos Aires, Argentina.

[b]UBA–CONICET, Facultad de Farmacia y Bioquímica, Instituto de Nanobiotecnología (NANOBIOTEC), Buenos Aires, Argentina.

[c]Universidad de Buenos Aires (UBA), Facultad de Farmacia y Bioquímica, Departamento de Microbiología, Inmunología, Biotecnología y Genética, Cátedra de Inmunología, Junín 956, C1113AAD Buenos Aires, Argentina.

[d]UBA–CONICET, Facultad de Farmacia y Bioquímica, Instituto de Estudios de la Inmunidad Humoral “Prof. Ricardo A. Margni” (IDEHU), Buenos Aires, Argentina.

[e]Trebe Biotech SRL. Ruta 8 km 225.5, Pergamino, Buenos Aires, Argentina.

[f]Unidad de Investigación y Desarrollo en Tecnología Farmacéutica (UNITEFA), CONICET. Departamento de Ciencias Farmacéuticas, Facultad de Ciencias Químicas, Universidad Nacional de Córdoba, Ciudad Universitaria, Córdoba 5000, Argentina.

***Corresponding author:**

Dr. Romina J. Glisoni

E-mail: rglisoni@ffyb.uba.ar; romy.glisoni@gmail.com

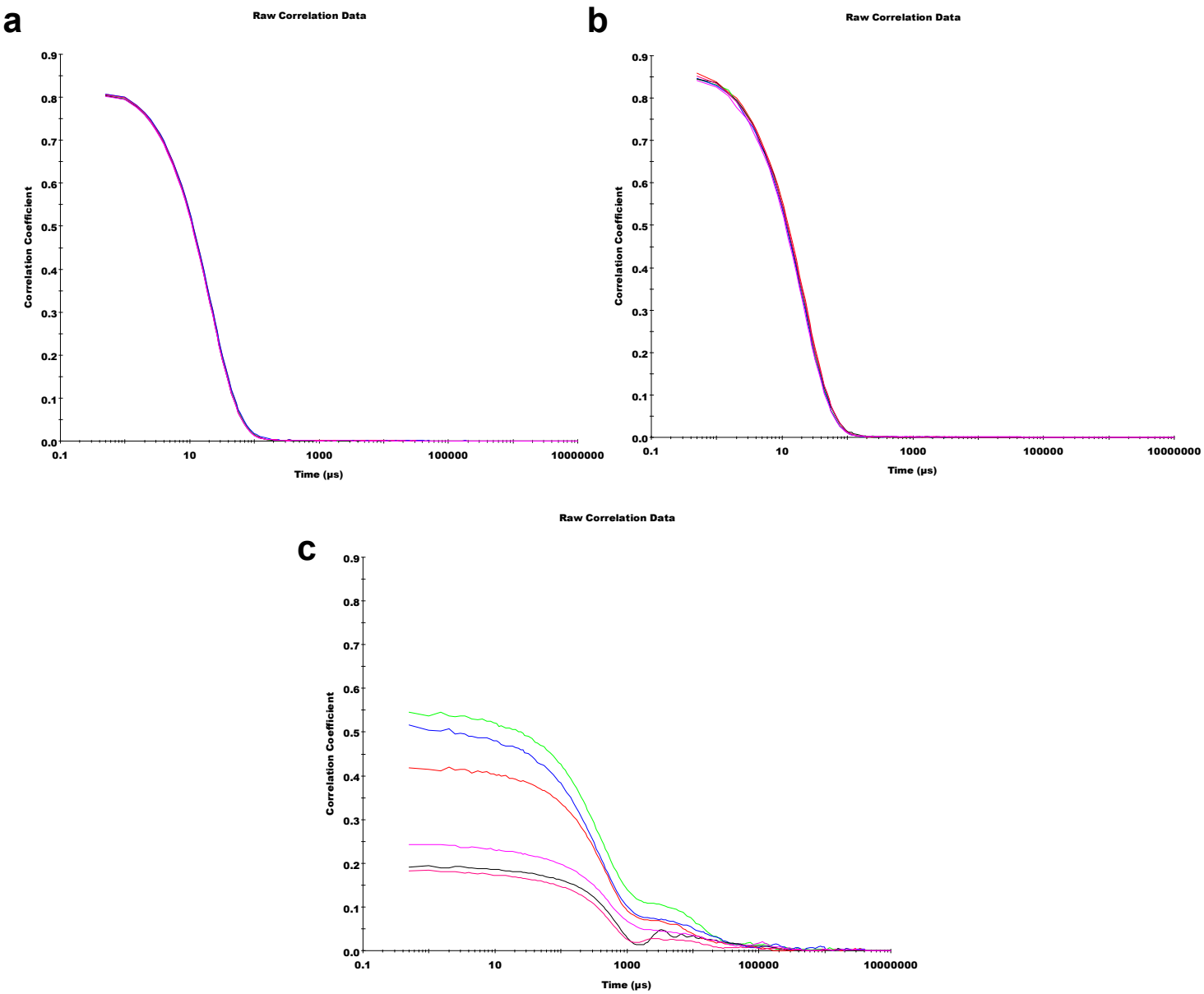

Fig. S1. Autocorrelation functions obtained by DLS for formulations dispersed in PBS and measured at 37 °C: (a) P123 PMs (2.5% w/v), (b) P123/QS-21 mixed PMs (2.5/0.02% w/v), and (c) free QS-21 (0.02% w/v). Autocorrelation functions were generated using Malvern Zetasizer software (v7.13). Data are representative of three independently prepared samples, each measured in six consecutive DLS runs.

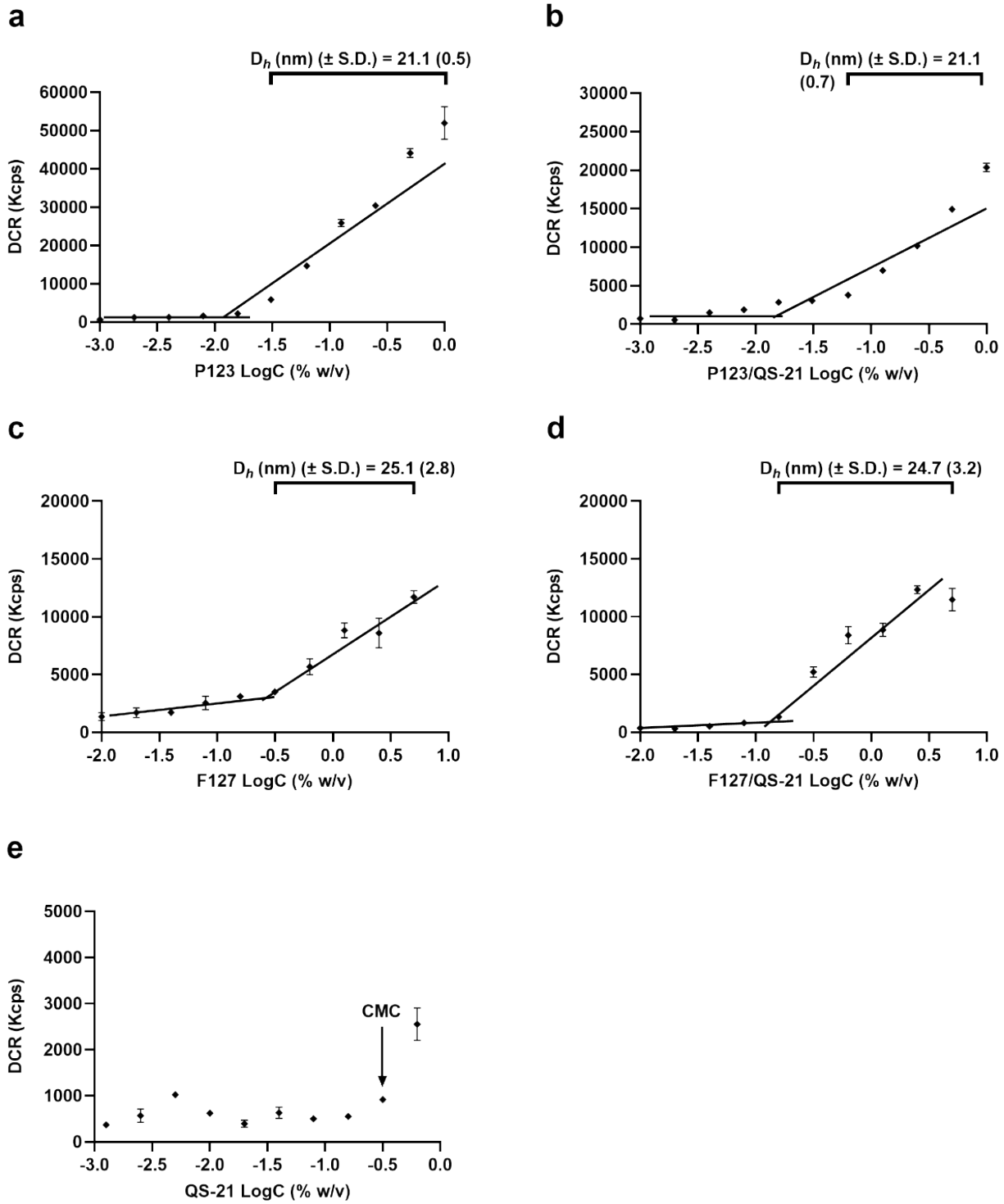

Fig. S2. Derived count rate (DCR), expressed as kilocounts per second (kcps), as a function of the logarithm of concentration for (a) pristine P123, (b) P123/QS-21, (c) pristine F127, and (d) F127/QS-21, and as a function of QS-21 concentration for free QS-21 (e), measured in PBS at 37 °C by DLS. The apparent CMC was defined as the inflection point corresponding to an abrupt increase in DCR. For panels a–d, the concentration ranges yielding single-mode particle populations and the corresponding stable hydrodynamic diameters (± S.D.) are indicated.

a

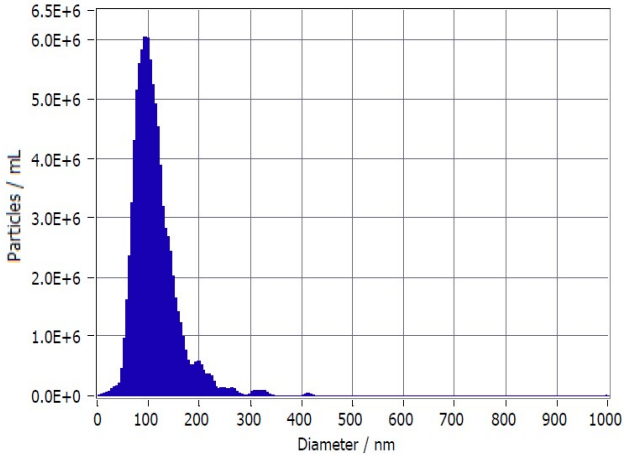
Particles / mL
6.5E+6
6.0E+6
5.0E+6
4.0E+6
3.0E+6
2.0E+6
1.0E+6
0.0E+0
0 100 200 300 400 500 600 700 800 900 1000
Diameter / nm

b

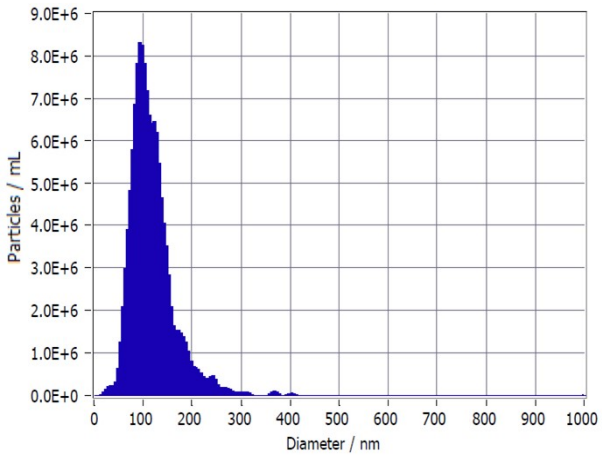
Particles / mL
9.0E+6
8.0E+6
7.0E+6
6.0E+6
5.0E+6
4.0E+6
3.0E+6
2.0E+6
1.0E+6
0.0E+0
0 100 200 300 400 500 600 700 800 900 1000
Diameter / nm

c

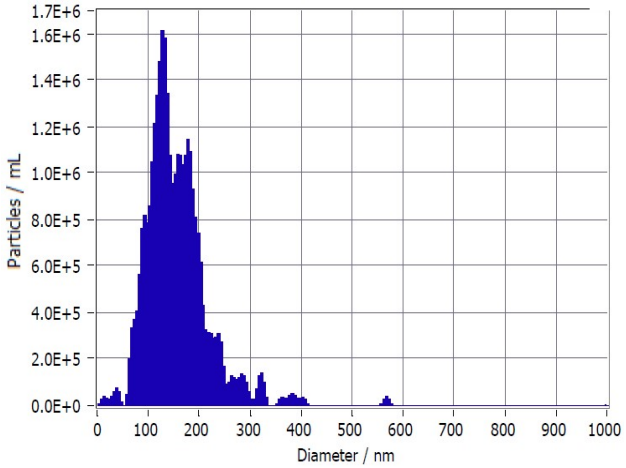
Particles / mL
1.7E+6
1.6E+6
1.4E+6
1.2E+6
1.0E+6
8.0E+5
6.0E+5
4.0E+5
2.0E+5
0.0E+0
0 100 200 300 400 500 600 700 800 900 1000
Diameter / nm

d

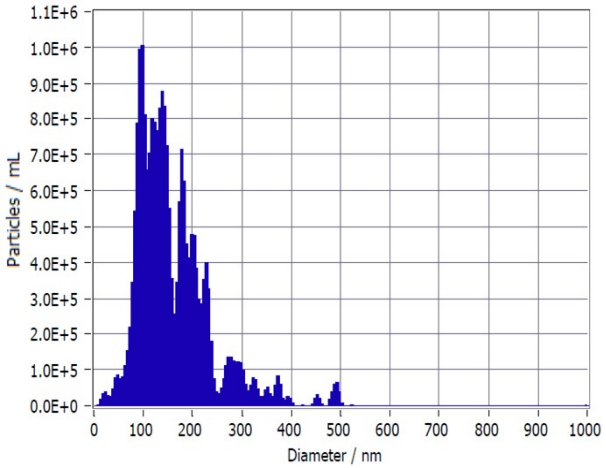
Particles / mL
1.1E+6
1.0E+6
9.0E+5
8.0E+5
7.0E+5
6.0E+5
5.0E+5
4.0E+5
3.0E+5
2.0E+5
1.0E+5
0.0E+0
0 100 200 300 400 500 600 700 800 900 1000
Diameter / nm

Fig. S3. Particle concentration (particles mL^{-1}) as a function of hydrodynamic diameter (nm) for (a) pristine P123, (b) P123/QS-21, (c) pristine F127, and (d) F127/QS-21 formulations, measured at 25 °C by NTA. Data were extracted directly from ZetaView software (version 8.05.16 SP7).

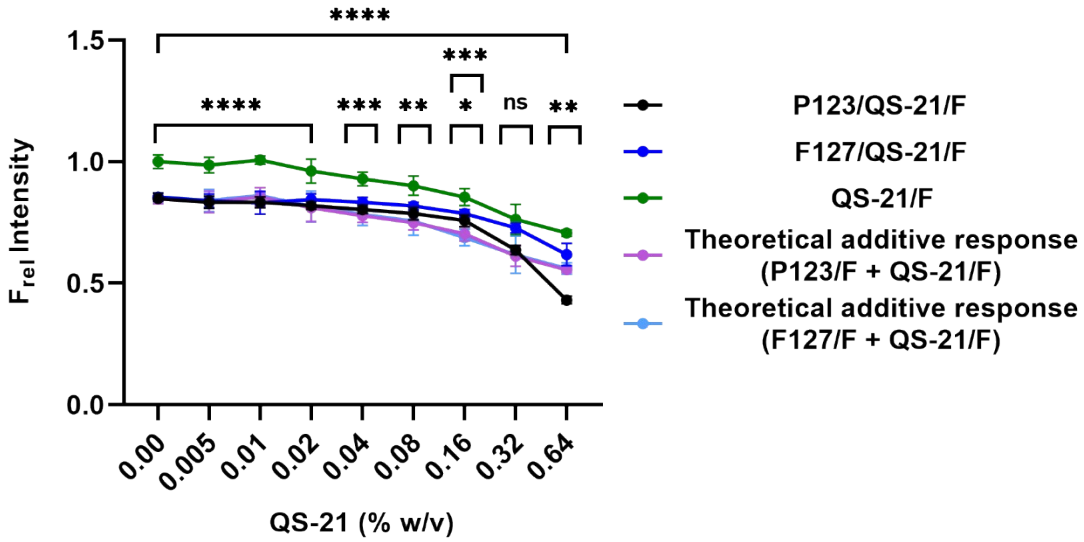

Fig. S4. Relative fluorescence intensity (F_{rel} Intensity) of fluorescein (F) in P123/QS-21/F and F127/QS-21/F systems (2.5% w/v copolymer, 0.00–0.64% w/v QS-21 and 0.5 μM F), and QS-21/F (0.00–0.64% w/v/0.5 μM F) in PBS, along with the corresponding theoretical additive response of their individual components. F_{rel} Intensity values are expressed relative to free F (0.5 μM) in PBS. Samples were incubated at 37 °C for 30 min prior to measurement. Excitation and emission wavelengths were set at 455 and 515 nm, respectively. Measurements were performed using a gain of 85 and 15 flashes per point, after subtraction

of the corresponding blank. The curve corresponding to the “Theoretical additive response” represents the calculated response under the assumption of independent contributions of the copolymer (P123 or F127) and QS-21. Data are presented as mean ± S.D. (n = 3). Statistical analysis was performed using two-way ANOVA, followed by Bonferroni’s multiple comparison test. Statistical significance is indicated as ns (not significant), *$p < 0.05$, **$p < 0.01$, ***$p < 0.001$, and ****$p < 0.0001$. Upper brackets correspond to comparisons between QS-21/F and P123/QS-21/F, while lower brackets correspond to comparisons between QS-21/F and F127/QS-21/F at each QS-21 concentration (% w/v).

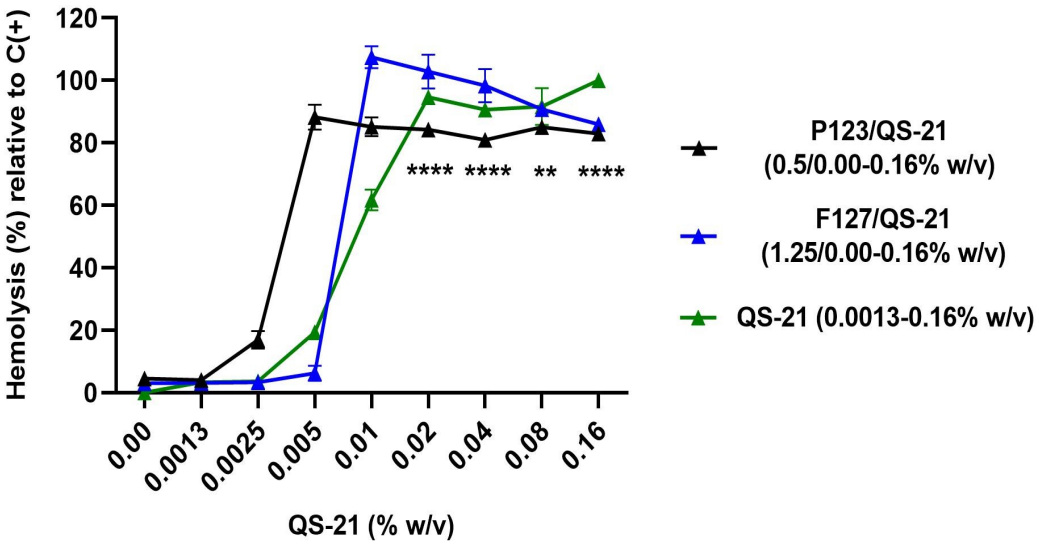

Fig. S5. Hemolytic activity expressed as hemolysis (%) relative to the positive control (C(+), defined as 100% hemolysis) as a function of QS-21 concentration (% w/v). Hemolysis was evaluated for P123/QS-21 and F127/QS-21 mixed PMs containing 0.5% and 1.25% (w/v) of each copolymer, respectively, with QS-21 concentrations ranging from 0.00–0.16% (w/v), as well as for free QS-21 over the concentration range 0.0013–0.16% (w/v). Data are presented as mean ± S.D. Statistical analysis was performed

using two-way ANOVA, followed by Bonferroni's multiple comparison test. Statistical comparisons correspond to differences between each formulation and free QS-21 at equivalent concentrations. Reductions in hemolytic activity relative to free QS-21 were observed for P123/QS-21 PMs in the QS-21 concentration range 0.02–0.16% (w/v) and for F127/QS-21 at 0.16% (w/v). Statistical significance is indicated as $^{**}p < 0.01$ and $^{****}p < 0.0001$.

Video S1 (AVI). NTA representative frame recording of P123/QS-21 mixed PMs in PBS at 25 °C, showing fast Brownian motion and a homogeneous nanoscale particle population.

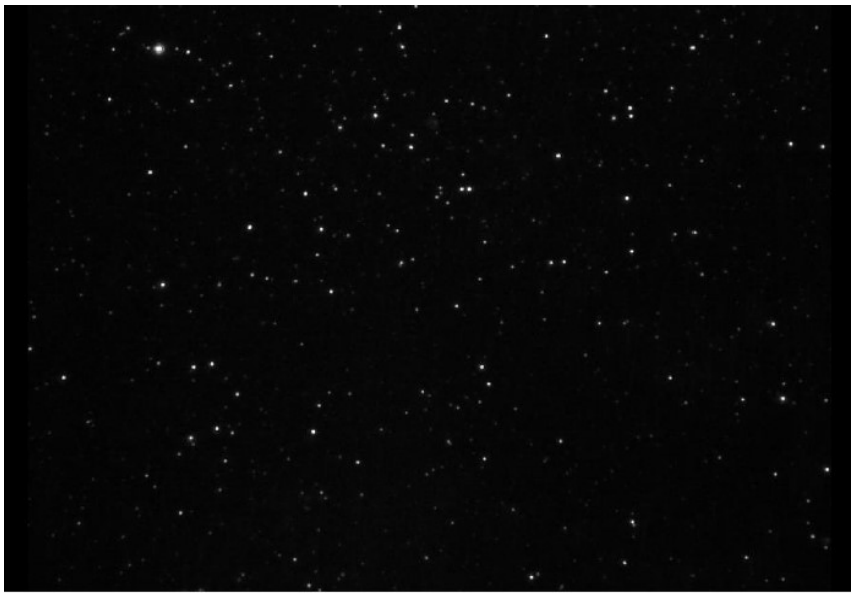

Video S2 (AVI). NTA representative frame recording of F127/QS-21 mixed PMs in PBS at 25 °C, showing slower Brownian motion and fewer detectable

scattering entities, consistent with the lower effective particle number density determined by NTA.